Received: 28 March 2023 | Revised: 4 May 2023 | Accepted: 7 May 2023

DOI: 10.1002/jmor.21598

RESEARCH ARTICLE

JOURNAL OF morphology WILEY

Evolutionary traces of miniaturization in a giant—Comparative anatomy of brain and brain nerves in *Bathochordaeus stygius* (Tunicata, Appendicularia)

Berit Zemann[1] | **Mai-Lee Van Le**[2] | **Rob E. Sherlock**[3] | **Daniel Baum**[4] | **Kakani Katija**[3] | **Thomas Stach**[2]

[1]Museum für Naturkunde, Berlin, Germany

[2]Humboldt-Universität zu Berlin, Vergleichende Elektronenmikroskopie, Berlin, Germany

[3]Monterey Bay Aquarium Research Institute, Moss Landing, California, USA

[4]Zuse-Institut Berlin, Berlin, Germany

Correspondence
Thomas Stach, Humboldt-Universität zu Berlin, Vergleichende Elektronenmikroskopie Berlin 10099, Germany.
Email: thomas.stach@hu-berlin.de

Funding information
Deutsche Forschungsgemeinschaft; David and Lucile Packard Foundation

Abstract

Appendicularia comprises 70 marine, invertebrate, chordate species. Appendicularians play important ecological and evolutionary roles, yet their morphological disparity remains understudied. Most appendicularians are small, develop rapidly, and with a stereotyped cell lineage, leading to the hypothesis that Appendicularia derived progenetically from an ascidian-like ancestor. Here, we describe the detailed anatomy of the central nervous system of *Bathochordaeus stygius*, a giant appendicularian from the mesopelagic. We show that the brain consists of a forebrain with on average smaller and more uniform cells and a hindbrain, in which cell shapes and sizes vary to a greater extent. Cell count for the brain was 102. We demonstrate the presence of three paired brain nerves. Brain nerve 1 traces into the epidermis of the upper lip region and consists of several fibers with some supportive bulb cells in its course. Brain nerve 2 innervates oral sensory organs and brain nerve 3 innervates the ciliary ring of the gill slits and lateral epidermis. Brain nerve 3 is asymmetric, with the right nerve consisting of two neurites originating posterior to the left one that contains three neurites. Similarities and differences to the anatomy of the brain of the model species *Oikopleura dioica* are discussed. We interpret the small number of cells in the brain of *B. stygius* as an evolutionary trace of miniaturization and conclude that giant appendicularians evolved from a small, progenetic ancestor that secondarily increased in size within Appendicularia.

KEYWORDS
comparative anatomy, invertebrate morphology, molecular systematics, phylogenetics

Berit Zemann and Mai-Lee Van Le contributed equally to this study.

1 | INTRODUCTION

Appendicularians are a small group of exclusively marine chordates, with approximately 70 known species (Fenaux, 1998; Fenaux et al., 1998; Hopcroft, 2005). As planktonic chordates feeding on picoplankton, appendicularians occupy pivotal positions in ecological food webs and in the evolutionary tree of life (Gorsky & Fenaux, 1998; Lombard et al., 2011). With their complex houses acting as filters (e.g., Flood, 1991, 1994, Katija et al., 2020; Razghandi et al., 2021), appendicularians concentrate the surrounding seawater by approximately a factor of 1000, before ingesting the filtrate. Consequently, appendicularians efficiently remove particles from the seawater as small as 160 nm, including bacteria and viruses (Lawrence et al., 2018). Preyed upon by numerous larger animals including cnidarians, ctenophores, chaetognaths, and fishes (Miller et al., 2011; Purcell, 2003; Spriet, 1997), appendicularians form a crucial link that channels organic material from the submicron range into the oceanic food web, bypassing the microbial loop. Since appendicularian houses are regularly discarded and rapidly sink to the bottom, they remove carbon directly from the photic zone and indirectly, yet effectively, from the atmosphere (Berline et al., 2011; Hansen et al., 1996; Katija et al., 2017). Indeed, appendicularian houses can in certain areas contribute up to 83% of the total carbon deposited to the sea floor (Alldredge et al., 2005). Since the houses of giant appendicularians like *Bathochordaeus* spp. are underrepresented by conventional sampling methods, their role in carbon flux estimates has not been accounted for historically (Robison et al., 2005).

The peculiar feeding mechanism of appendicularians requires a finely tuned regulation of tail beats and arrests (Conley et al., 2018; Selander & Tiselius, 2003). Most animals can also reject unwanted particles by temporarily detaching the mouth from the buccal tube of the house and reversing the direction of the ciliary beat in the gill slits (Deibel, 1986; Fenaux, 1986). In addition, discarding a house, swimming, and inflating a new house requires completely different movements (Glover, 2020; Lohmann, 1933; Spriet, 1997). These complex behaviors are coordinated by a nervous system, consisting of a central brain and peripheral nerves, that innervate musculature, cilia, and epidermis or receive input from sensory cells.

Taxonomically, Appendicularia belongs to Tunicata, the possible sister taxon of Craniota and is therefore important for understanding the early evolution of vertebrates (Braun et al., 2020; Delsuc et al., 2006). Unlike other tunicates, appendicularians retain the body division into trunk and postanal tail throughout their lives. In this, they resemble larval ascidians and appendicularians are accordingly also called larvaceans. As most appendicularians are small, develop rapidly, and with a stereotyped cell lineage, it has been suggested that they evolved through heterochrony from an ancestor with a free-swimming tadpole-like larva and a sessile, ascidian-like adult (Garstang, 1928; Stach et al., 2008; Stach & Turbeville, 2005). According to this hypothesis, the heterochronic, more specifically progenetic, miniaturization of appendicularians constitutes an apomorphic feature. Alternatively, it had been suggested that swimming freely represented a plesiomorphic trait inherited unaltered from the last common ancestor of Chordata (Swalla et al., 2000; Wada, 1998). The latter hypothesis is based on the hypothesis that Appendicularia was the sister taxon to all remaining Tunicata, a phylogenetic position that has since been recovered consistently in molecular phylogenetic studies (Delsuc et al., 2018; Kocot et al., 2018) and also in a cladistic analysis of morphological characters (Braun et al., 2020).

From meso- and bathypelagic zones several appendicularian species are known. With a trunk length of up to 25 mm, they are considerably larger than appendicularians from the photic epipelagic zone (Chun, 1900; Fenaux & Youngbluth, 1990; Sherlock, Walz, Robison, et al., 2016; Sherlock, Walz, Schlining, et al., 2016). Morphologically, little is known of these giant appendicularians beyond their original species descriptions (Garstang, 1937; Lohmann, 1933). In this study, we investigated *Bathochordaeus stygius* Garstang, 1937, a giant appendicularian from the Eastern Pacific, to expand the knowledge of the morphological disparity of appendicularians. Moreover, this study allowed us to identify anatomical traces of miniaturization in the nervous system of *B. stygius* from which we conclude that giant appendicularians evolved from a small, progenetic ancestor that secondarily increased in size within Appendicularia.

2 | MATERIALS AND METHODS

Two specimens of *B. stygius* were collected from MBARI (Monterey Bay Aquarium Research Institute, California, USA) using a remotely operated vehicle, *Ventana*, and gentle suction (see Table 1; Robison, 1993). Animals showed normal regular tail beat and were healthy looking, undamaged, corresponding to the description and depictions rendered in the species description by Garstang (1937; Figure 1a,b and Supporting Information: Figures S1 and S2). Animals were maintained alive until they could be fixed onshore using a solution of 1% paraformaldehyde, 2.5% glutaraldehyde in 0.2 mol l^{-1} sodium cacodylate buffer (pH 7.2), and adjusted to an osmolarity of approximately 800 mOsm with the addition of sodium chloride. Primary fixation was stopped after 1 h with three buffer rinses. Animals were stored in the same buffer and shipped in the buffer via express mail to the Laboratory of Comparative Electron Microscopy at Humboldt University (Berlin, Germany). Here, animals were postfixed in a solution of 1% osmium tetroxide (OsO_4) in double-distilled water

TABLE 1 Collection details for *Bathochordaeus stygius* specimens.

Individual	Collection date	Geographic coordinates of sampling	Sampling depth (m)
Specimen 1	09/18/2019	N 36.7477 W −122.10454	135
Specimen 2	11/08/2019	N 36.7448 W −122.1014	312

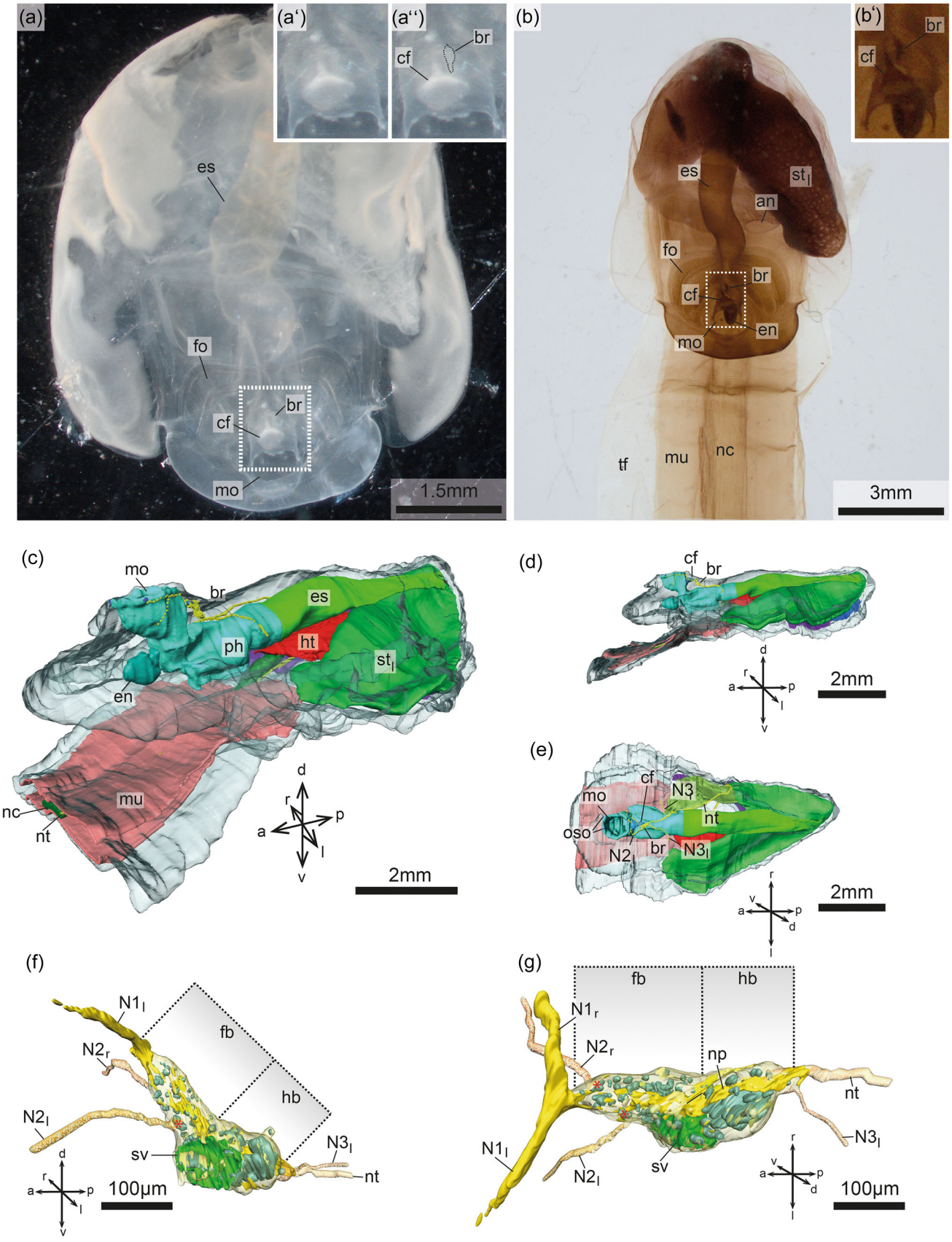

FIGURE 1 (See caption on next page)

(ddH_2O). Postfixation was stopped with three rinses (once for 15 and twice for 30 min) with ddH_2O. One specimen was used for microcomputed tomography (μCT) analysis using an XRadia Versa 410 X-ray microscope (Carl Zeiss Microscopy GmbH; see Supporting Information: Figure S2). After dehydration through a graded series of ethanol, the second specimen was embedded in Araldite. A complete transverse series of semithin (2.0 μm thick) sections was sectioned of the trunk for light microscopy (Leica Ultracut S), resulting in 4529 sections. Semithin sections were stained for 15–20 min with toluidine blue. About 6% of the 4529 sections prepared for our analysis were either folded or partly rolled up and could therefore not be analyzed in detail. Light microscopic images were recorded with a digital camera (Canon EOS 700D) mounted on a Zeiss Axioplan compound microscope. Every 12th section was recorded (distance, 24 μm) using the ×2.5 objective lense for the three-dimensional (3D) reconstruction of the anatomy of the complete trunk. Additionally, every section was recorded (distance, 2.0 μm) using the ×40 objective for the 3D reconstruction of the detailed anatomy of the brain and adjacent parts of the brain nerves. Light micrographs of details were recorded with a ×100 oil-immersion objective. Based on the resulting stack of images, 3D models of the complete trunk showing the anatomy of all organ systems and of the brain were reconstructed using the software Amira 6.4.0 (Thermo Fisher Scientific). For the anatomical 3D model of the trunk, organs and tissues were segmented. For the detailed reconstruction of the brain, individual cells (where possible) and individual nuclei were traced and segmented. The diameter of cells and nuclei in the forebrain and hindbrain regions was measured directly on the micrographs; every fifth micrograph was used for the measurement. Volumes of cells and nuclei were calculated in Amira ZIB Edition 2023.04 with the Label Analysis module (Thermo Fisher Scientific, Zuse-Institut Berlin). Further analysis was realized with the Filter Analysis module filtering for volumes of cells larger and smaller than 15,000 μm^3 as well as for volumes of nuclei larger and smaller than 1600 μm^3. The resulting label fields were visualized as surfaces generated with the Generate Surface module.

The second 3D reconstruction was created in the same way, based on the image stack of the μCT-analysis. While this data set has the advantages of being based on a high number of optimally aligned optical sections (1181; voxel size 12.8 μm) and not having the specimen potentially deformed during embedding, the μCT-imaging does not allow for a histological distinction of the different tissues. Thus, the resulting model is on the one hand smoother and more live-like in outer appearance and some of the major organ systems and at the same time contains less information on their substructure or even no information (e.g., the pericardium; see Supporting Information: Figure 2).

3 | RESULTS

Upon capture, animals showed normal regular tail beats and appeared healthy looking, undamaged, corresponding to the description and depictions rendered in the species description by Garstang (1937; Figure 1a,b and Supporting Information: Figures S1 and S2). Histological preservation of our specimens, however, was suboptimal, showing empty vesicles or signs of swelling on the one hand, but detailed preservations, such as cilia, microvilli, or single neurites, on the other hand. This indicates that our preservation regime favored cells and tissues rich in structural proteins. In our opinion, the difficulties involved in securing giant appendicularians for science justify presenting suboptimal histological sections, especially since virtually nothing is known about the histology of these animals.

Like in all appendicularians, the body of *B. stygius* is divided into a trunk and a tail. However, compared to other appendicularians, the trunk is not only considerably larger but also broad, dorsoventrally flattened, and features a dorsally directed mouth opening (Figure 1a–e). The brain is positioned in the sagittal midline, dorsal to the pharynx, approximately 200 μm posterior to the mouth (Figure 1). To the right of the brain extends the ciliary funnel that anteriorly opens into the posterior wall of the mouth cavity. In lateral view, the brain is roughly pear-shaped (Figure 1f). The longitudinal axis of the brain aligns approximately with the dorsoventral axis of the trunk. The brain is about 220 μm in length and the ventral broader base measures around 140 μm, whereas at the dorsal tip, the brain is merely 20–30 μm wide. In dorsal view, the brain of *B. stygius* is more spindle-shaped with a slightly broader posterior part (Figure 1g). This broader posterior part extends over two-thirds of the length of the brain and bulges toward the left side (Figure 1f,g). The brain is attached to the ciliary funnel via a ribbon-shaped extension of the basement membrane (Figure 2d). Similarly, another, more sheet-like structure extends from the left side of the brain into the hemocoel (Figure 2c–e).

FIGURE 1 Three-dimensional (3D) reconstruction of the anatomy of *Bathochordaeus stygius*. (a) Low-power micrograph of the trunk of an individual of *B. stygius* after glutaraldehyde fixation in dorsal view. Insets a′ and a″ show higher magnification of the area marked with a stippled rectangle in (a). (b) Low-power micrograph of the trunk and part of the tail of a second individual of *B. stygius* after glutaraldehyde fixation and OsO_4 postfixation in dorsal view. Inset (b′) shows a higher magnification of the area marked with stippled rectangle in (b). (c) Overview of the anatomy of the trunk and part of the tail in oblique lateral view. 3D reconstruction. (d) Overview of the anatomy of the trunk and part of the tail in lateral view from the left side. (e) Overview of the anatomy of the trunk and part of the tail in dorsal view. (f) Brain, brain nerves, and nuclei in lateral view from the left side. (g) Brain, brain nerves, and nuclei in oblique dorsal view. br, brain; cf, ciliated funnel; es, esophagus; fb, forebrain; fo, Fol's oikoplast; hb, hindbrain; ht, heart pericard; mo, mouth opening; mu, musculature; $N1_{l/r}$, left/right first brain nerve; $N2_{l/r}$, left/right second brain nerve; $N3_l$, left third brain nerve; oso, oral sensory organ; nc, notochord; np, neuropil; nt, nerve cord; stl, left stomach lobe; sv, sensory vesicle; tf, tail fin; red asterisks, nuclei of second brain nerves.

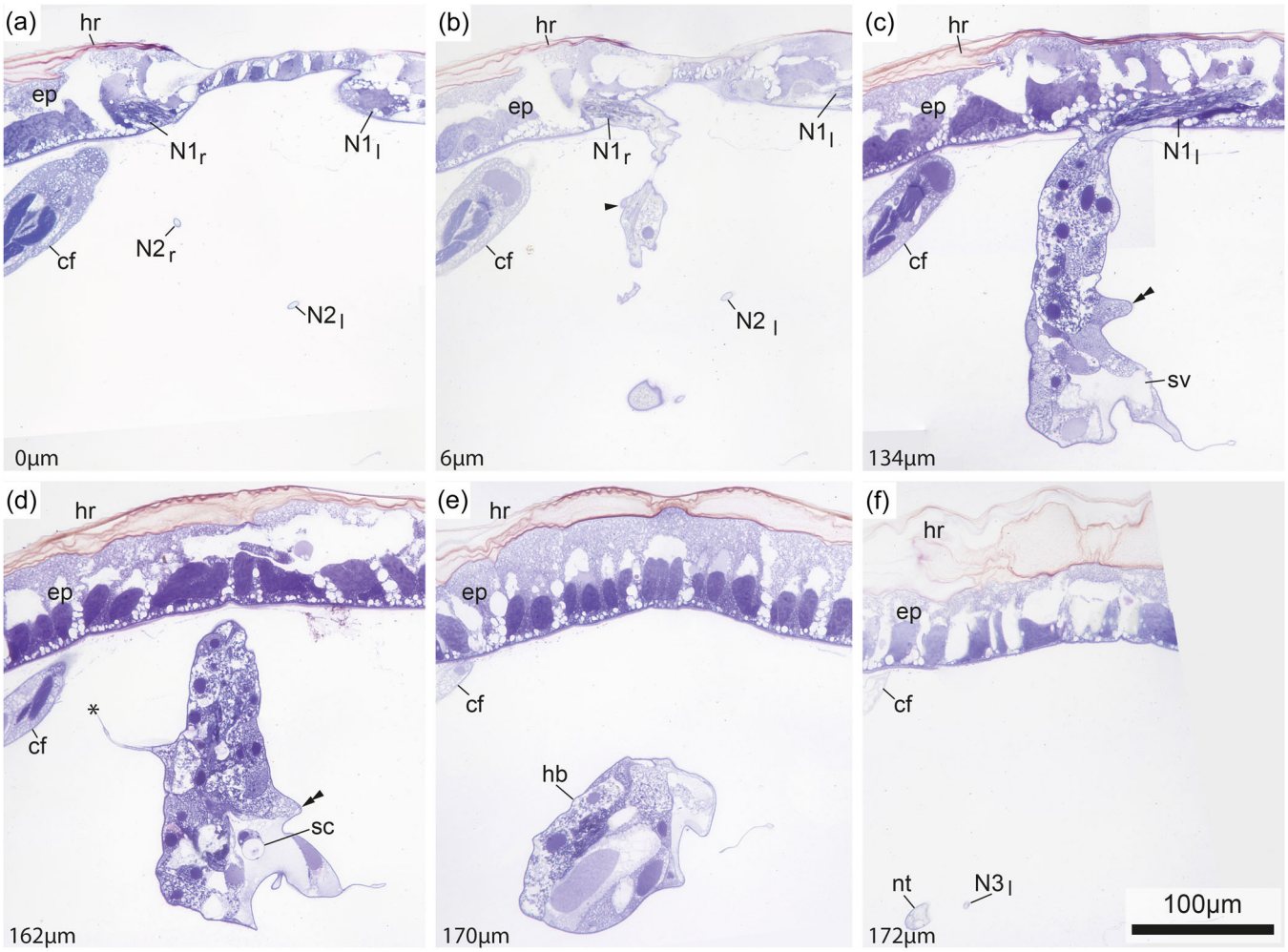

FIGURE 2 Light micrographs of consecutive cross-sections of the brain of *Bathochordaeus stygius*. Sections are from anterior (a) to posterior (f). Images are selected from a complete series of sections. The distance from the first section shown in (a) is indicated in the lower left corner of each image. cf, ciliated funnel; ep, epidermis; hb, hindbrain; hr, house rudiment; sc, statocyst; $N1_{l/r}$, left/right first brain nerve; $N2_l$, left second brain nerve; $N3_l$, left third brain nerve.

Morphologically, the brain can be divided into an anterior part ("forebrain") and a posterior part ("hindbrain"; Figures 1 and 3). This division corresponds to a slight dorsoventral bend in lateral view (Figure 1f and 3a,c) and a slight restriction in circumference between the broader hindbrain and the narrower forebrain in dorsal view (Figure 1g and 3d,e). On the left side, from the posterior part of the forebrain along most part of the hindbrain, the brain contains the sensory vesicle with a conspicuous statocyst (Figure 2d and Supporting Information: Figure S3). Fiber tracts, that is, a neuropil area, can be traced through the posterior part of the forebrain, the hindbrain, and into the nerve cord (Figures 1g, 2, and 4).

The forebrain makes up the anterior two-thirds of the brain in length. It contains 67 cells identified by their nuclei (Figure 3 and Table 2). Cell boundaries could be identified for 55 of the forebrain cells. These cells in the forebrain range in diameter from approximately 12–27 µm. They have an average volume of 7006 µm^3 that ranges from 1202 to 25,767 µm^3. In general, the nuclei of the cells in the forebrain are similar in size, ranging from 5 to 13 µm in diameter, with a mean of nearly 9 µm. They are uniformly colored and dark blue in light micrographs. They are markedly distinguished from the coarsely mottled cytoplasm that is light blue in coloration (Figures 2c and 4a). Nuclei in the forebrain have an average volume of 681 µm^3 that ranges from 116 to 1631 µm^3.

In the posterior part of the brain, we unambiguously identified 35 cells (see Table 2). Again, some cell membranes could not be identified with certainty, although the presence of several nuclei indicates that separate cells were present. The cells in the hindbrain differ considerably from the more uniform cells in the forebrain. The size of the cells in the hindbrain ranges from a diameter of about 16 µm to almost 100 µm in diameter in cross-sections (Figure 4b). This broad range is mirrored in the volumes of the cells that range from 1820 to 137,928 µm^3 with an average of 23,880 µm^3. The three largest cells range in volume between 77,909 and 137,928 µm^3. In addition, the shapes of the hindbrain cells are not as uniform as those of the forebrain cells. Hindbrain cells are elongated in sections, dorsoventrally flattened, and with irregular bulges. Nuclei of these

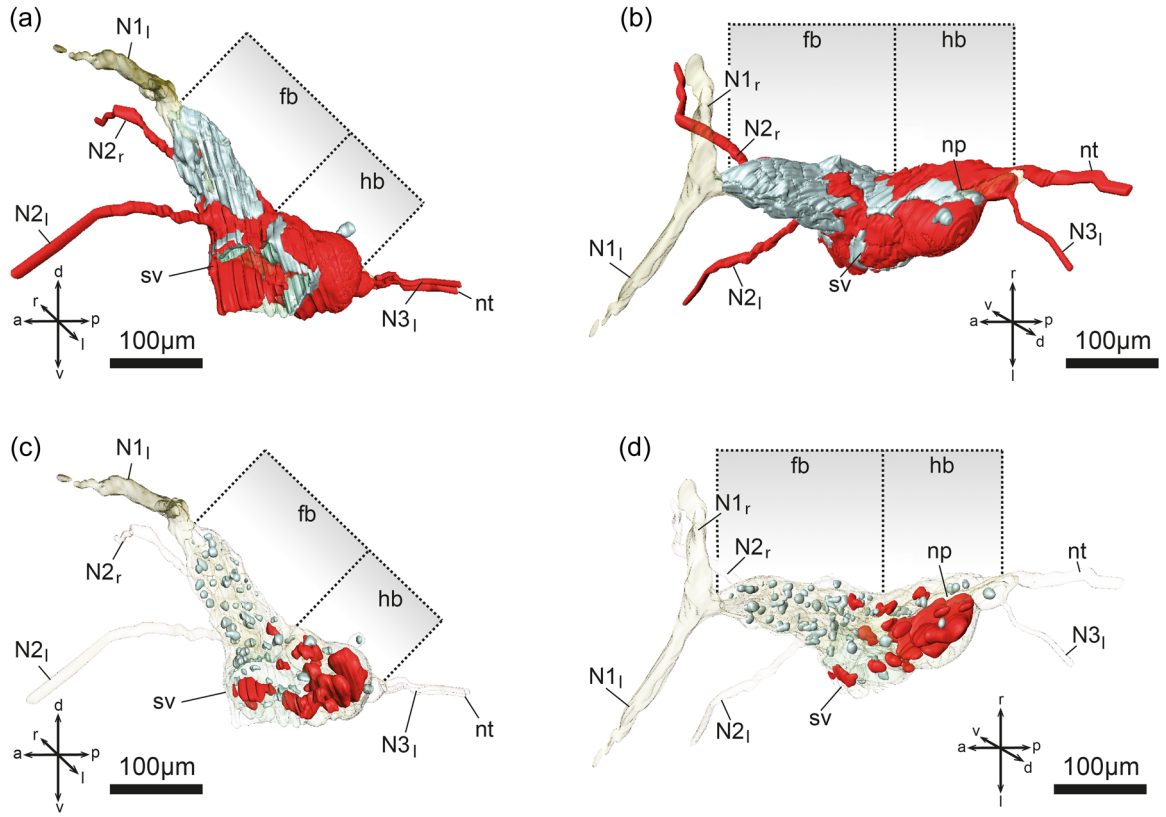

FIGURE 3 Three-dimensional (3D) reconstruction of the brain of *Bathochordaeus stygius*. (a and b) In gray: Cells with a volume less than 12,600 µm^3. In red: Cells with a volume of 15,600 µm^3 and more. (a) Brain and brain nerves in lateral view from the left side. (b) Brain and brain nerves in oblique dorsal view. (c and d) In gray: Nuclei with a volume less than 1480 µm^3. In red: Nuclei with a volume of 1630 µm^3 and more. (c) Brain and brain nerves in lateral view from the left side. (d) Brain and brain nerves in oblique dorsal view. fb, forebrain; hb, hindbrain; $N1_{l/r}$, left/right first brain nerve; $N2_{l/r}$, left/right second brain nerve; $N3_l$, left third brain nerve; np, neuropil; nt, nerve cord; sv, sensory vesicle.

cells are also irregular in shape and substantially larger than those in the anterior brain, measuring up to 74 µm along the longer sectional axis. Nuclei in the hindbrain have an average volume of 4487 µm^3 that ranges from 320 to 40,436 µm^3. Histologically, the cells are more variable than the cells in the forebrain. Staining varies from a light, grayish blue to dark blue, almost violet. The cytoplasm in some cells is of a smooth, fine appearance, while in other hindbrain cells, the cytoplasm is coarsely granulated (Figures 2e and 4b).

The sensory vesicle is situated on the left side of the posterior third of the brain. It consists of a fluid-filled cavity that contains a statocyte (Figure 2c,d and Supporting Information: Figure S3). The nucleus and cytoplasm of the statocyte lie directly adjacent to the large statolith. The statolith is perfectly circular in cross-section, with a diameter of about 20 µm (Figure 2d and Supporting Information: Figure 3). The sensory vesicle is lined by cells that in some places appear fragmented. We counted 15 nuclei of cells lining the sensory vesicle, 11 on the medial side bordering the main part of the brain and 4 laterally, adjacent to the hemocoel. The overall irregular outline of the sensory vesicle in our micrographs suggests that it collapsed during the fixation process.

Several nerves and neurites leave (respectively enter) the brain, and posteriorly, the brain extends into the nerve cord or nerve cord (Figures 1–3 and 5). The most prominent and most voluminous nerve leaving the brain is the most anterior first brain nerve. It is a paired nerve that bifurcates immediately after leaving the brain anteriorly. The first brain nerve is composed of numerous neurites (Figures 2a–c and 6). It extends over a distance of approximately 110 µm on each side and contacts epidermis cells at the posterior side of the mouth opening. Outside the brain, some cell somata are closely placed alongside the first brain nerve (Figure 6a–c; Supporting Information: Figure 4). These somata are, therefore, located in the basal part of the dorsal epidermis posterior to the mouth opening. Three such somata could be identified in the first brain nerve on the right side, and two somata in the first brain nerve on the left side.

Some 40 µm posterior to the first brain nerve, the second brain nerve that is also paired leaves the brain ventrally in the anterior direction (Figures 1f,g, 2a,d, 5, and 6e). In fact, the second brain nerve on the right side leaves the brain slightly anterior to its left counterpart. The nerves consist of a single neurite that runs underneath the epidermis around the mouth opening. The right second brain nerve, therefore, passes between the ciliary funnel and the epidermis. The somata giving rise to the second brain nerves are situated in the anterior part of the forebrain (Figure 1f,g). The neurites of the second brain nerves eventually branch with a short

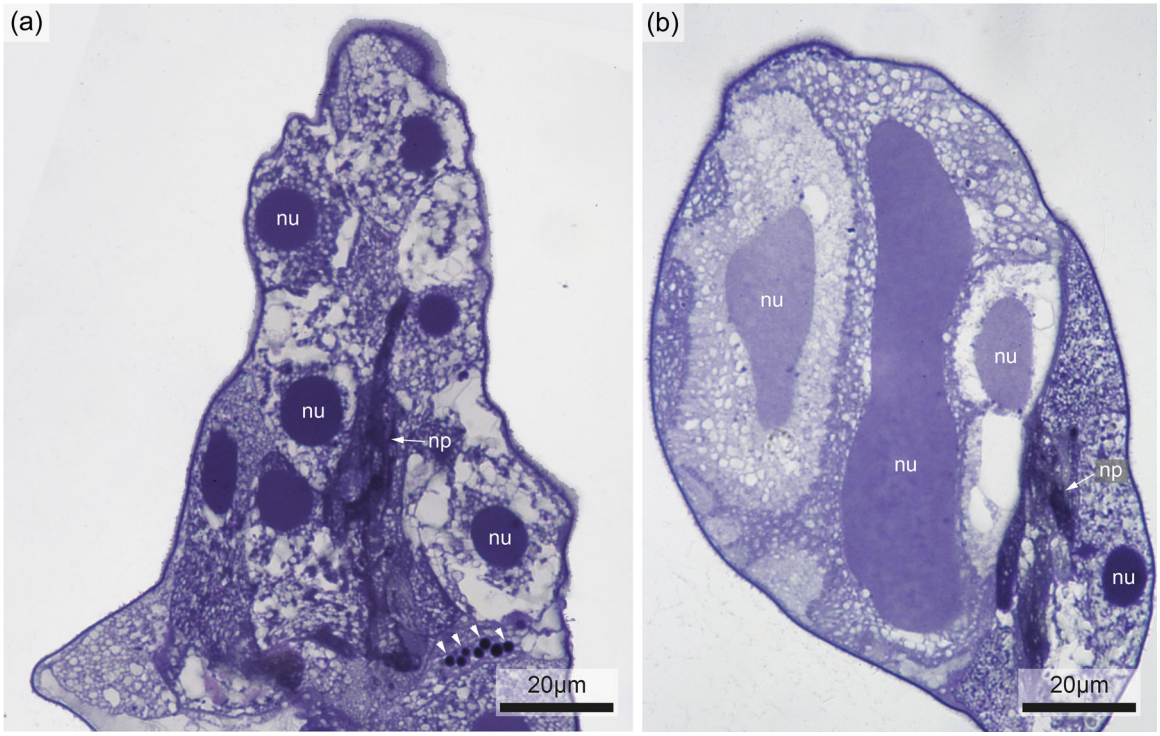

FIGURE 4 Light micrographs of cross-sections through the brain of *Bathochordaeus stygius*. Note uniformly dark-stained vesicles in the cell ventral in the forebrain (arrowheads). (a) Forebrain and (b) hindbrain. np, neuropil; nu, nucleus.

TABLE 2 Meristic characteristics of cells in the anterior versus the posterior brain region.

	No. of cells	∅ Cells' diameter (µm)	Range cells' diameter (µm)	∅ Cells' volume (µm^3)	Range cells' volume (µm^3)	∅ Nuclei diameter (µm)	Range nuclei diameter (µm)	∅ Nuclei volume (µm^3)	Range nuclei volume (µm^3)
Forebrain	67	19.4	12.5–26.8	7006	1202–25,767	8.6	5.1–13.1	681	116–1631
Hindbrain	35	35.9	16.0–99.8	23,880	1820–137,928	18.2	6.3–74.1	4487	320–40,436

branch running dorsally to the epidermis of the posterior margin of the mouth opening. The other branch continues anteriorly, branches some more times, and contacts three complex oral sensory organs situated in the epithelium of the lateral and anterior margin of the mouth and the anterior part of the mouth cavity (Figures 5 and 7) on each side.

The left third brain nerve and the nerve cord leave the brain together, the brain nerve just left of the nerve cord. Different from the other brain nerves, the third brain nerve is asymmetrical (Figures 1e–g and 5). Its counterpart on the right side is part of the nerve cord and branches off from the rest of the nerve cord about 500 µm posterior to the brain. Nevertheless, we will call this right-sided nerve "right third brain nerve." The third brain nerve consists of three neurites on the left side (Figure 8a,b) and two neurites on the right side. Both third brain nerves branch into a ramus branchialis that runs toward the elongated ciliated rings of the gill slits on each side and another branch (ramus epidermalis) that projects toward the adjacent lateral epidermis (Figures 5 and 8).

4 | DISCUSSION

Most of our knowledge about appendicularians is generalized from detailed studies of *Oikopleura dioica* (Ferrández-Roldán et al., 2019). This is true for molecular, developmental, and ecological studies, but even for morphological or evolutionary studies. In *O. dioica* the brain consists of 78–150 cells (Braun & Stach, 2019; Glover, 2020; Nishida et al., 2021; Søviknes et al., 2005; see also Supporting Information: Table 1), which—like the small size and the high developmental speed among other things—have been considered as indications of neotenic acceleration during evolution (e.g., Garstang, 1928; Stach et al., 2008; Stach & Turbeville, 2005).

The anatomy of the nervous system in several *Oikopleura* species has been investigated by light microscopy (Lohmann, 1933; Martini, 1909a, 1909b) and details of the anatomy of the brain have been investigated by electron microscopy in *O. dioica* (Nishida et al., 2021; Olsson et al., 1990). We showed that details of the anatomy of the nervous system in the mesopelagic giant *B. stygius* correspond to morphological structures described for *Oikopleura* spp.,

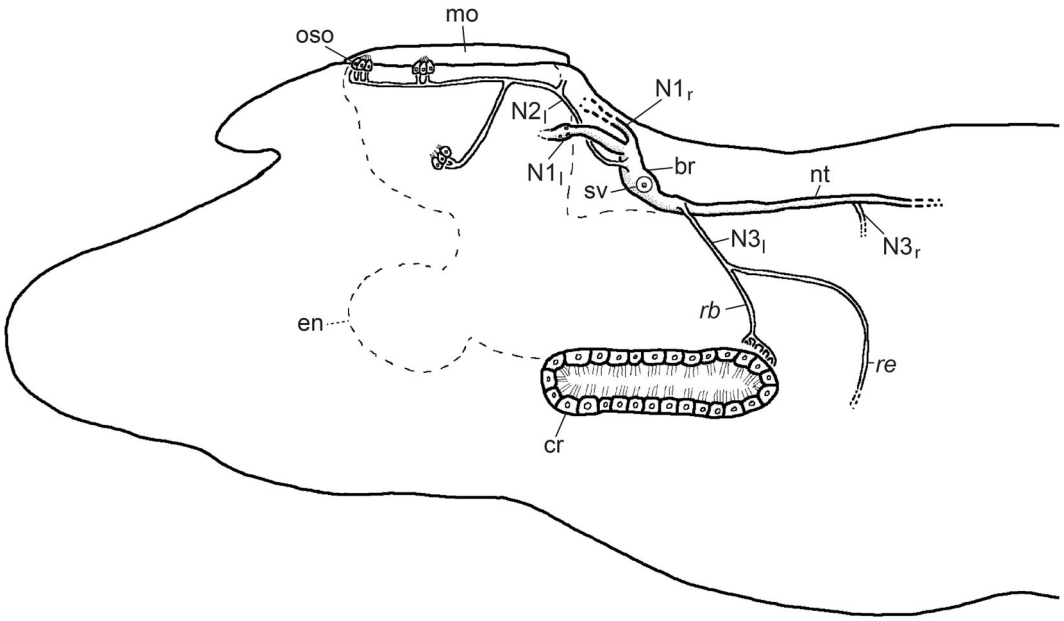

FIGURE 5 Semischematic drawing of the brain, brain nerves, and their targets in *Bathochordaeus stygius*. Anterior is to the left and dorsal is to the top. cr, ciliary ring; en, endostyle; mo, mouth opening; $N1_{l/r}$, left/right first brain nerve; $N2_{l}$, left second brain nerve; $N3_{l/r}$, left/right third brain nerve; oso, oral sensory organ; rb, ramus branchialis (of the left third brain nerve); re, ramus epidermalis (of the left third brain nerve).

but at the same time revealed notable differences. Like in *Oikopleura* spp., the first pair of brain nerves consists of several fibers that leave the brain anteriorly. Also, each of the first brain nerves features nuclei outside the brain, belonging to a small group of cells that were called bulb cells by Bollner et al. (1986) and supportive cells by Nishida et al. (2021). Different from *Oikopleura* spp., however, the first brain nerves in *B. stygius* project into the epidermis of the posterior rim of the mouth. This corresponds to the upper lip region in *Oikopleura* spp. In contrast, in *Oikopleura* spp., the first pair of brain nerves project into the conspicuous ventral sense organs that in turn consist of 30 cells, each with a single conspicuous sensory cilium (Bollner et al., 1986) and are situated laterally on the ventral side of the animal. No such organs, or indeed ciliated sensory cells, are found in *B. stygius* in the region of the first brain nerves. Instead, the epidermis cells in that region are covered by the house rudiment and therefore seem to be part of the oikoplastic epithelium. The ventral sense organ in *O. dioica* has been shown to derive from a placode-like thickening during development (Bassham & Postlethwait, 2005). This anterior placode expresses some of the genes that are also expressed in the olfactory placode of vertebrates, such as *eyeA*, *six1/2*, or *pitx* (Bassham & Postlethwait, 2005; Mazet, 2006). Interestingly, the expression domain of these genes is ring-like around the future mouth opening in early hatchlings of *O. dioica*. Thus, it is possible that the first brain nerve in *B. stygius* projects to the upper lip area, but this region may still develop from the epidermal placode with the same ontogenetic expression profile.

The second brain nerve in *O. dioica* consists of a single neurite that contacts a specialized epidermal cell in the upper lip and several multiciliated secondary sensory cells around the mouth (Olsson et al., 1990). Olsson et al. (1990) categorized these sensory cells into lower lip cells and pharyngeal cells, but Morita et al. (2020), Nishida et al. (2021), and Rigon et al. (2013) demonstrated conclusively that the multiciliated secondary sensory cells form a ring around the mouth opening and constitute the coronal organ. Similar to the course and innervation pattern of the second brain nerve in *O. dioica*, the second brain nerve in *B. stygius* branches into a short ramus that projects into the upper lip area and a ventral branch that innervates sensory cells in the anterolateral mouth cavity and the anterior rim of the mouth opening that corresponds to the ventral lip area in *Oikopleura* spp. We could not identify the target of the dorsal ramus; other microscopic techniques such as electron microscopy based on serial ultrathin sections or confocal laser scanning microscopy could resolve this question. Like in *O. dioica*, the ventral branch of the second brain nerve contacts sensory, ciliated cells in *B. stygius*. Several dozens of these sensory cells, however, are organized in three oral sensory organs on each side (Mai-Lee Van Le [personal observation]). In *O. dioica*, the perikarya of the second brain nerves are situated in the forebrain and function as master neurons of the ciliary beat reversal in the ciliated rings of the gill slits (Olsson et al., 1990). Given the structural similarities in *B. stygius*, it is plausible to assume that the second brain nerves serve a corresponding function in this species.

In *O. dioica*, the third brain nerve of the different sides of the body differs; it contains two neurites on the right side and three on the left (Olsson et al., 1990). While we could show that the left third brain nerve in *B. stygius* consists of three neurites as well, we were unable to show the number of neurites in the right counterpart. Like in *O. dioica*, however, we could trace the neurites of the third brain nerves to the region of the ciliary rings of the gill slits and the lateral epidermis. Light microscopy, however, does not

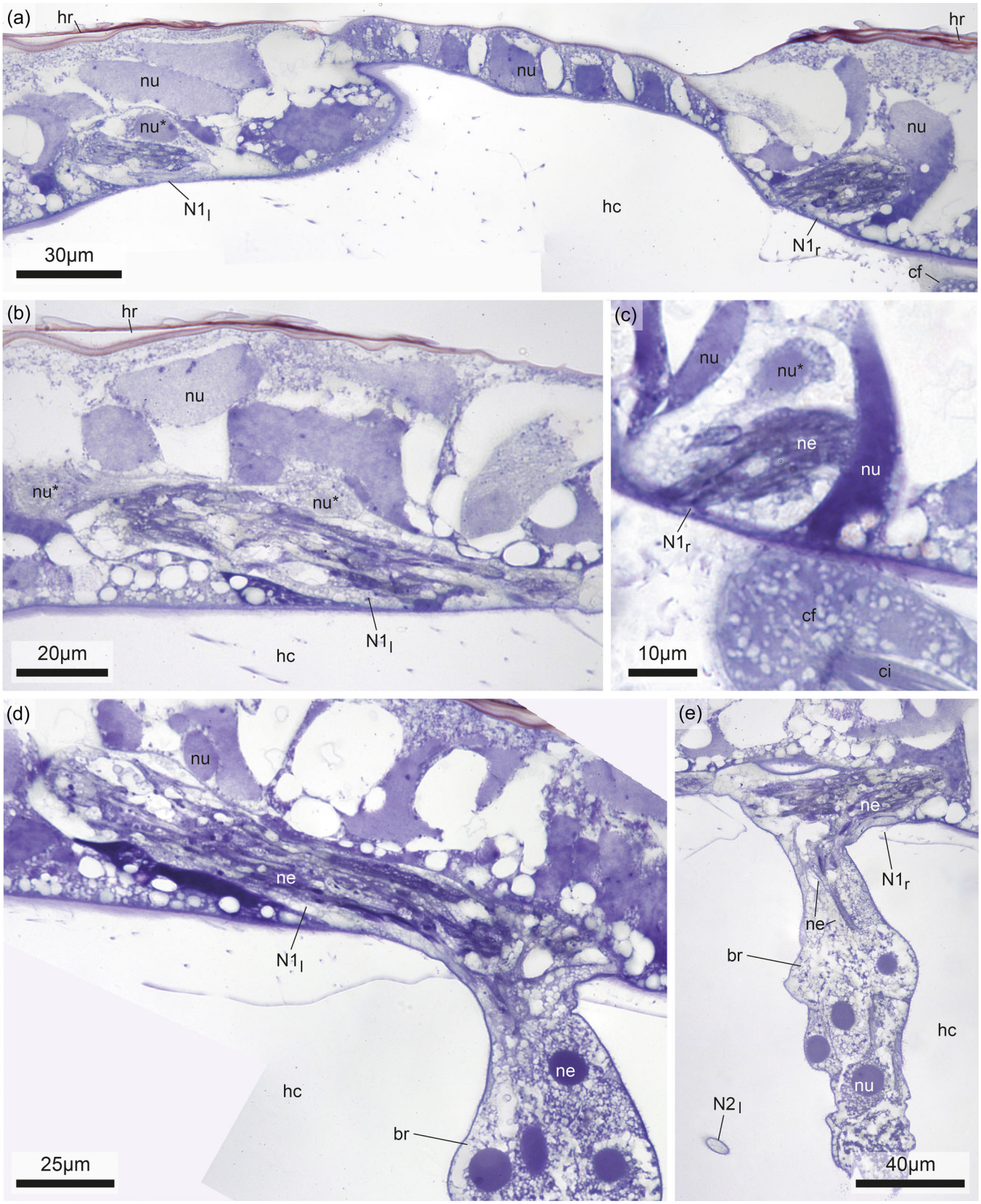

FIGURE 6 Light micrographic details of the pair of first brain nerves. Sections are from anterior (a) to posterior (e). Dorsal is to the top of the images. (a) Left and right first brain nerve in the dorsal epidermis; note the nucleus of one of the nerve cells in the left first brain nerve. (b) Two nuclei are seen in the left first brain nerve. (c) Note the nucleus in the right anterior brain nerve. (d) Neurites of the left anterior brain nerve entering the brain anteriorly. (e) Neurites of the right anterior brain nerve entering the brain anteriorly. c, ciliated funnel; ci, cilia; hr, house rudiment; ne, neurites; nu, nucleus; nu*, nucleus in the first brain nerve; $N1_{l/r}$, left/right first brain nerve.

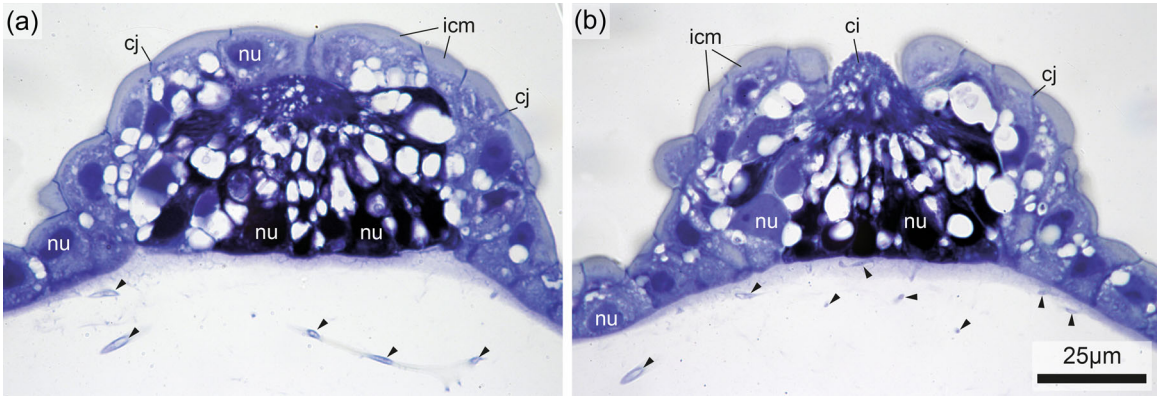

FIGURE 7 Light micrographs (a, b) showing terminal branches of the left second brain nerve (arrowheads) close to the ciliated sensory cells in one of the oral sensory organs of *Bathochordaeus stygius*. Dorsal is to the top of the images. br, brain; ci, cilia; cj, cell junction; hc, hemocoel; icm, intracellular matrix; nu, nucleus.

suffice to demonstrate synaptic contacts; transmission electron microscopy or specific labeling would be necessary for validation. The pair of third brain nerves differs from *O. dioica* in another aspect as well; the third brain nerve in *B. stygius* does not leave the brain directly (and therefore by definition does not constitute a brain nerve). Instead, it accompanies the nerve cord for about 500 µm before branching off toward the right gill slit and epidermis, demonstrating at the same time evolutionary plasticity and constancy.

Different from *O dioica*, we did not find a pair of dorsal neurites projecting into the dorsal oikoplastic epidermis (Cañestro et al., 2005; Olsson et al., 1990). These neurites might be lacking in *B. stygius*, they might be incorporated into the first brain nerve, or we may have missed these neurites due to the technique used in the present study because these neurites might have been on sections, we were unable to analyze.

Earlier molecular phylogenetic results positioned Appendicularia as the sister taxon to the remaining tunicates and concluded that the last common ancestor of Tunicata was a free-living, swimming organism (e.g., Wada, 1998). This hypothesis contrasted with the more traditional hypotheses that regarded Appendicularia as an evolutionarily progenetic form derived from a sessile tunicate ancestor with a tadpole larva (Garstang, 1928; review in Stach & Turbeville, 2005). This "progenesis hypothesis" (also neoteny hypothesis or pedomorphosis) was based on several observations:

(i) features that are larval in ascidians, such as the tail or the statocyst, are present in adult appendicularians (Cañestro et al., 2005; Garstang, 1928; Lohmann, 1933);
(ii) ontogenetic events, for example, cell fate determination or gastrulation, occur comparatively early in appendicularians (Delsman, 1910, 1912; Nishida & Stach, 2014; Stach et al., 2008);
(iii) most appendicularians are miniaturized, that is, they show a body size comparable to ascidian larvae at sexual maturity;
(iv) appendicularians show eutely (constancy in cell numbers) in several (but not all) tissues (Kishi et al., 2017; Nishida et al., 2021; Søviknes et al., 2007), a trait that is thought to be correlated with miniaturization.

With a trunk length larger than 1 cm, and an overall body size of 3–4 cm, species in the genus *Bathochordaeus* have been called giant appendicularians and in size are more similar to many solitary ascidians or cephalochordates (e.g., Kott, 1985; Poss & Boschung, 1996; Shenkar & Swalla, 2011). Could this be a plesiomorphic trait for Appendicularia? A brain length of approximately 220 µm in *B. stygius* is twice the brain length observed in *O. dioica* (Braun & Stach, 2019), while the trunk length of *B. stygius* is approximately 50 times larger than in *O. dioica* (ca. 500 µm trunk length at maturity). At the same time, the cell numbers in the brains are similar (ca. 78–150 in *O. dioica*, a cell count of 102 in *B. stygius* in the present study; see also Supporting Information: Table 1). This cell number is probably close to the minimum number necessary to perform the complex behaviors of appendicularians detailed above. Thus, we suggest that the miniaturized brain of the giant appendicularians is a plesiomorphic feature within Appendicularia. In other words, *B. stygius*' small brain with its small number of cells is an indication that giant appendicularians evolved from smaller appendicularian ancestors and secondarily became larger. A similar argument has recently been proposed concerning the evolution of genome sizes within Appendicularia (Naville et al., 2019). In addition, the dorsal direction of the mouth supports this hypothesis: while in the smaller appendicularians the mouth opening is in line with the longitudinal axis of the trunk as in ascidians, vertebrates, and adult cephalochordates, it is directed upwards in *B. stygius*, that is, at a right angle with the longitudinal axis of the trunk. At the same time, the remaining intestinal tract follows a u-shaped course in *B. stygius*, like in ascidians and the smaller appendicularians. According to this hypothesis (Figure 9), the mouth of giant appendicularians changed its position from terminal to dorsal during evolution as already suggested by Garstang when describing *B. stygius* as a species in

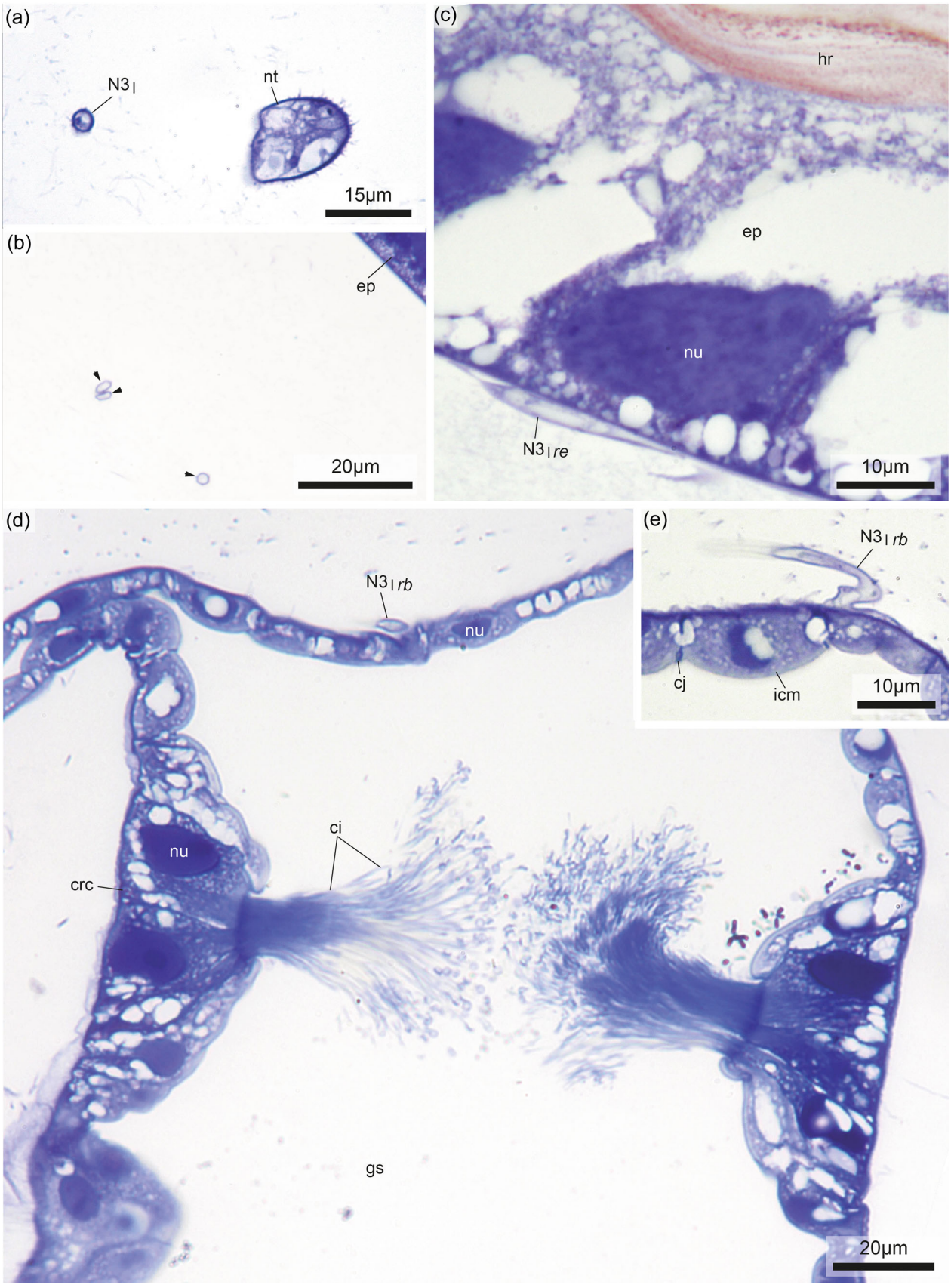

FIGURE 8 (See caption on next page)

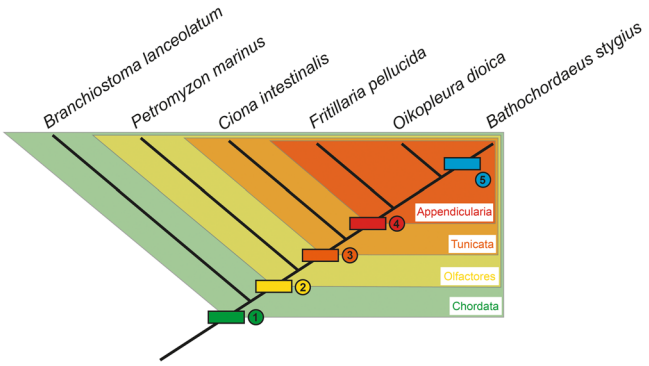

FIGURE 9 Phylogenetic relationship of selected chordate representatives combined after several authors. Apomorphies that evolved in the stem lineages marked by colored and numbered rectangles include: ① notochord, nerve cord/neural tube, endostyle; ② molecular characters; ③ tunic with cellulose, heartbeat reversal; ④ external filtering house, rotation, and translocation of tail, miniaturization, progenesis; ⑤ dorsal translocation of mouth, increase in body size (but not brain), invasion of mesopelagial.

1937. The orientation of the longitudinal axis of the brain close to a right angle as compared to the longitudinal axis of the trunk shows that the brain paralleled the evolutionary transformation of the mouth.

AUTHOR CONTRIBUTIONS

Berit Zemann: Investigation; visualization; formal analysis; data curation; writing—review and editing. **Mai-Lee Van Le**: Conceptualization; investigation; validation; visualization; formal analysis; data curation; supervision. **Rob E. Sherlock**: Resources; writing—review and editing. **Daniel Baum**: Software; writing—review and editing. **Kakani Katija**: Resources; funding acquisition; writing—review and editing. **Thomas Stach**: Conceptualization; funding acquisition; supervision; project administration; validation; Writing - original draft.

ACKNOWLEDGMENTS

This work was supported by DFG Grant Number STA 655/11–1 and the David and Lucile Packard Foundation. We are deeply indebted to Dr. Christian Wirkner (University of Rostock) for the preparation of the µCT scan of one of the *B. stygius* specimens used for this study.

DATA AVAILABILITY STATEMENT

All data are publicly available upon request.

ORCID

Rob E. Sherlock http://orcid.org/0000-0002-5474-9880
Kakani Katija http://orcid.org/0000-0002-7249-0147
Thomas Stach http://orcid.org/0000-0001-5461-9069

PEER REVIEW

The peer review history for this article is available at https://www.webofscience.com/api/gateway/wos/peer-review/10.1002/jmor.21598.

REFERENCES

Alldredge, A. L., Gorsky, G., Youngbluth, M., & Deibel, D. (2005). The contribution of discarded appendicularian houses to the flux of particulate organic carbon from oceanic surface waters. In G. Gorsky, M. J. Youngbluth, & D. Deibel (Eds.), *Response of marine ecosystems to global change: Ecological impact of appendicularians* (pp. 309–326). Éditions scientifiques GB.

Bassham, S., & Postlethwait, J. H. (2005). The evolutionary history of placodes: A molecular genetic investigation of the larvacean urochordate *Oikopleura dioica*. *Development*, *132*, 4259–4272.

Berline, L., Stemmann, L., Vichi, M., Lombard, F., & Gorsky, G. (2011). Impact of appendicularians on detritus and export fluxes: A model approach at DyFAMed site. *Journal of Plankton Research*, *33*, 855–872.

Bollner, T., Holmberg, K., & Olsson, R. (1986). A rostral sensory mechanism in *Oikopleura dioica* (Appendicularia). *Acta Zoologica*, *67*, 235–241.

Braun, K., Leubner, F., & Stach, T. (2020). Phylogenetic analysis of phenotypic characters of Tunicata supports basal Appendicularia and monophyletic Ascidiacea. *Cladistics*, *36*, 259–300.

Braun, K., & Stach, T. (2019). Morphology and evolution of the central nervous system in adult tunicates. *Journal of Zoological Systematics and Evolutionary Research*, *57*, 323–344.

Cañestro, C., Bassham, S., & Postlethwait, J. (2005). Development of the central nervous system in the larvacean *Oikopleura dioica* and the evolution of the chordate brain. *Developmental Biology*, *285*, 298–315.

Chun, C. (1900). *Aus den Tiefen des Weltmeeres* (Vol. 1900, pp. 519–521). Gustav Fischer.

Conley, K. R., Gemmell, B. J., Bouquet, J. M., Thompson, E. M., & Sutherland, K. R. (2018). A self-cleaning biological filter: How appendicularians mechanically control particle adhesion and removal. *Limnology and Oceanography*, *63*, 927–938.

Deibel, D. (1986). Feeding mechanism and house of the appendicularian *Oikopleura vanhoeffeni*. *Marine Biology*, *93*, 429–436.

Delsman, H. C. (1910). Beiträge zur Entwicklungsgeschichte von *Oikopleura dioica*. *Verh Rijksinst Onderzoek der Zee*, *3*, 3–24.

Delsman, H. C. (1912). Weitere Beobachtungen über die Entwicklung von *Oikopleura dioica*. *Tijdschr Ned Dierk Ver (Ser 2)*, *12*, 197–215.

Delsuc, F., Brinkmann, H., Chourrout, D., & Philippe, H. (2006). Tunicates and not cephalochordates are the closest living relatives of vertebrates. *Nature*, *439*, 965–968.

Delsuc, F., Philippe, H., Tsagkogeorga, G., Simion, P., Tilak, M.-K., Turon, X., López-Legentil, S., Piette, J., Lemaire, P., &

FIGURE 8 Light micrographic details of the third brain nerve of *Bathochordaeus stygius*. Dorsal is to the top of images. (a) Third brain nerve on the left side next to the nerve cord. (b) Left third brain nerve immediately after the branching into the ramus branchialis (two neurites) and the ramus epidermalis (one neurite). (c) Ramus epidermalis of the left third brain nerve running underneath the lateral epidermis. (d) Ramus branchialis of the left third brain nerve close to the ciliary ring cells of the left gill slit. (e) Enlarged light micrograph of the ramus branchialis of the left third brain nerve close to the ciliary ring cells of the left gill slit. ci, cilia; cj, cell junction; crc, ciliary ring cell; ep, epidermis; gs, gill slit; hr, house rudiment; icm, intracellular matrix; $N3_{l\ rb}$, ramus branchialis of the left third brain nerve; $N3_{l\ re}$, ramus epidermalis of the left third brain nerve; nu, nucleus; nt, nerve cord; arrowheads point to individual neurites.

Douzery, E. J. P. (2018). A phylogenomic framework and timescale for comparative studies of tunicates. *BMC Biology*, *16*, 39.

Fenaux, R. (1986). The house of *Oikopleura dioica* (Tunicata, Appendicularia): Structure and functions. *Zoomorphology*, *106*, 224–231.

Fenaux, R. (1998). Anatomy and functional morphology of the Appendicularia. In Q. Bone (Ed.), *The biology of pelagic Tunicates* (pp. 25–34). Oxford University Press.

Fenaux, R., Bone, Q., & Deibel, D. (1998). Appendicularian distribution and zoogeography. In Q. Bone (Ed.), *The biology of pelagic Tunicates* (pp. 251–264). Oxford University Press.

Fenaux, R., & Youngbluth, M. J. (1990). A new mesopelagic appendicularian, *Mesochordaeus bahamasi* gen. nov., sp. nov. *Journal of the Marine Biological Association of the United Kingdom*, *70*, 755–760.

Ferrández-Roldán, A., Martí-Solans, J., Cañestro, C., & Albalat, R. (2019). *Oikopleura dioica*: An emergent chordate model to study the impact of gene loss on the evolution of the mechanisms of development. In T. Tworzydlo, & S. M Bilinski (Eds.), *Evo-devo: Non-model species in cell and developmental biology* (pp. 63–105). Springer International Publishing.

Flood, P. R. (1991). Architecture of, and water circulation and flow rate in, the house of the planktonic tunicate *Oikopleura labradoriensis*. *Marine Biology*, *111*, 95–111.

Garstang, W. (1928). Memoirs: The morphology of the Tunicata, and its bearings on the phylogeny of the Chordata. *Journal of Cell Science*, *s2-72*, 51–187.

Garstang, W. (1937).). On the anatomy and relations of the Appendicularian *Bathochordaeus*, based on a new species from Bermuda (*B. stygius*, sp. n.). *Journal of the Linnean Society of London, Zoology*, *40*, 283–303.

Glover, J. C. (2020). Oikopleura. *Current Biology*, *30*, R1243–R1245.

Gorsky, G., & Fenaux, R. (1998). The role of Appendicularia in marine food webs. In Q. Bone (Ed.), *The biology of pelagic Tunicates* (pp. 161–169). Oxford University Press.

Hansen, J., Kiørboe, T., & Alldredge, A. (1996). Marine snow derived from abandoned larvacean houses: Sinking rates, particle content and mechanisms of aggregate formation. *Marine Ecology Progress Series*, *141*, 205–215.

Hopcroft, R. R. (2005). Diversity in larvaceans: How many species. In G. Gorsky, M. J. Youngbluth, & D. Deibel (Eds.), *Response of marine ecosystems to global change: Ecological impact of appendicularians* (pp. 45–57). Contemporary Publishing International.

Katija, K., Sherlock, R. E., Sherman, A. D., & Robison, B. H. (2017). New technology reveals the role of giant larvaceans in oceanic carbon cycling. *Science Advances*, *3*, e1602374.

Katija, K., Troni, G., Daniels, J., Lance, K., Sherlock, R. E., Sherman, A. D., & Robison, B. H. (2020). Revealing enigmatic mucus structures in the deep sea using DeepPIV. *Nature*, *583*, 78–82.

Kishi, K., Hayashi, M., Onuma, T. A., & Nishida, H. (2017). Patterning and morphogenesis of the intricate but stereotyped oikoplastic epidermis of the appendicularian, *Oikopleura dioica*. *Developmental Biology*, *428*, 245–257.

Kocot, K. M., Tassia, M. G., Halanych, K. M., & Swalla, B. J. (2018). Phylogenomics offers resolution of major tunicate relationships. *Molecular Phylogenetics and Evolution*, *121*, 166–173.

Kott, P. (1985). The Australian Ascidiacea. Part 1, Phlebobranchia and Stolidobranchia. *Memoirs of the Queensland Museum*, *23*, 1–440.

Lawrence, J., Töpper, J., Petelenz-Kurdziel, E., Bratbak, G., Larsen, A., Thompson, E., Troedsson, C., & Ray, J. L. (2018). Viruses on the menu: The appendicularian *Oikopleura dioica* efficiently removes viruses from seawater. *Limnology and Oceanography*, *63*, S244–S253.

Lohmann, H. (1933). *Erster Unterstamm der Chordata Tunicata—Manteltiere: Allgemeine Einleitung in die Naturgeschichte der Tunicata*. De Gruyter.

Lombard, F., Selander, E., & Kiørboe, T. (2011). Active prey rejection in the filter-feeding appendicularian *Oikopleura dioica*. *Limnology and Oceanography*, *56*, 1504–1512.

Martini, E. (1909a). Studien über Konstanz histologischer Elemente. 1. Oikopleura longicauda. *Zeitschrift für Wissenschaftliche Zoologie*, *92*, 563–626.

Martini, E. (1909b). Studien über Konstanz histologischer Elemente. 2. Fritillaria pellucida. *Zeitschrift für Wissenschaftliche Zoologie*, *94*, 81–170.

Mazet, F. (2006). The evolution of sensory placodes. *The Scientific World Journal*, *6*, 1841–1850.

Miller, M. J., Otake, T., Aoyama, J., Wouthuyzen, S., Suharti, S., Sugeha, H. Y., & Tsukamoto, K. (2011). Observations of gut contents of leptocephali in the North Equatorial Current and Tomini Bay, Indonesia. *Coastal Marine Science*, *35*, 277–288.

Morita, R., Onuma, T. A., Manni, L., Ohno, N., & Nishida, H. (2020). Mouth opening is mediated by separation of dorsal and ventral daughter cells of the lip precursor cells in the larvacean, *Oikopleura dioica*. *Development Genes and Evolution*, *230*, 315–327.

Naville, M., Henriet, S., Warren, I., Sumic, S., Reeve, M., Volff, J. N., & Chourrout, D. (2019). Massive changes of genome size driven by expansions of non-autonomous transposable elements. *Current Biology*, *29*(7), 1161–1168.e6.

Nishida, H., Ohno, N., Caicci, F., & Manni, L. (2021). 3D reconstruction of structures of hatched larva and young juvenile of the larvacean *Oikopleura dioica* using SBF-SEM. *Scientific Reports*, *11*, 4833.

Nishida, H., & Stach, T. (2014). Cell lineages and fate maps in tunicates: Conservation and modification. *Zoological Science*, *31*(10), 645–652.

Olsson, R., Holmberg, K., & Lilliemarck, Y. (1990). Fine structure of the brain and brain nerves of *Oikopleura dioica* (Urochordata, Appendicularia). *Zoomorphology*, *110*, 1–7.

Poss, S. G., & Boschung, H. T. (1996). Lancelets (Cephalochordata: Branchiostomattdae): How many species are valid? *Israel Journal of Zoology*, *42*(suppl 1), S13–S66.

Purcell, J. (2003). Predation on zooplankton by large jellyfish, Aurelia, Cyanea and Aequorea, in Prince William Sound, Alaska. *Marine Ecology Progress Series*, *246*, 137–152.

Razghandi, K., Janßen, N., Le, M. L. V., & Stach, T. (2021). The filter-house of the larvacean *Oikopleura dioica*. A complex extracellular architecture: From fiber production to rudimentary state to inflated house. *Journal of Morphology*, *282*, 1259–1273.

Rigon, F., Stach, T., Caicci, F., Gasparini, F., Burighel, P., & Manni, L. (2013). Evolutionary diversification of secondary mechanoreceptor cells in Tunicata. *BMC Evolutionary Biology*, *13*, 112.

Robison, B. H. (1993). Midwater research methods with MBARI's ROV. *Marine Technology Society Journal*, *26*, 32–39.

Robison, B. H., Reisenbichler, K. R., & Sherlock, R. E. (2005). Giant larvacean houses: Rapid carbon transport to the deep sea floor. *Science*, *308*, 1609–1611.

Selander, E., & Tiselius, P. (2003). Effects of food concentration on the behaviour of *Oikopleura dioica*. *Marine Biology*, *142*, 263–270.

Shenkar, N., & Swalla, B. J. (2011). Global diversity of Ascidiacea. *PLoS One*, *6*, e20657.

Sherlock, R. E., Walz, K. R., & Robison, B. H. (2016). The first definitive record of the giant larvacean, *Bathochordaeus charon*, since its original description in 1900 and a range extension to the northeast Pacific Ocean. *Marine Biodiversity Records*, *9*, 1–10.

Sherlock, R. E., Walz, K. R., Schlining, K. L., & Robison, B. H. (2016). Morphology, ecology, and molecular biology of a new species of giant larvacean in the eastern North Pacific: *Bathochordaeus mcnutti* sp. nov. *Marine Biology*, *164*, 1–15.

Spriet, E. (1997). *Studies on the house building epithelium of Oikopleurid appendicularia (Tunicata): Early differentiation and description of the adult pattern of oikoplast cells* (Master's thesis, The University of Bergen).

Stach, T., & Turbeville, J. M. (2005). The role of appendicularians in chordate evolution—A phylogenetic analysis of molecular and morphological characters, with remarks on "neoteny scenarios. In G. Gorsky, M. J. Youngbluth, & D. Deibel (Eds.), *Ecological impact of appendicularians* (pp. 9–26). Contemporary Publishing International.

Stach, T., Winter, J., Bouquet, J. M., Chourrout, D., & Schnabel, R. (2008). Embryology of a planktonic tunicate reveals traces of sessility. *Proceedings of the National Academy of Sciences of the United States of America*, *105*, 7229–7234.

Swalla, B. J., Cameron, C. B., Corley, L. S., & Garey, J. R. (2000). Urochordates are monophyletic within the deuterostomes. *Systematic Biology*, *49*, 52–64.

Søviknes, A. M., Chourrout, D., & Glover, J. C. (2005). Development of putative GABAergic neurons in the appendicularian urochordate *Oikopleura dioica*. *The Journal of Comparative Neurology*, *490*(1), 12–28.

Søviknes, A. M., Chourrout, D., & Glover, J. C. (2007). Development of the caudal nerve cord, motoneurons, and muscle innervation in the appendicularian urochordate *Oikopleura dioica*. *The Journal of Comparative Neurology*, *503*, 224–243.

Wada, H. (1998). Evolutionary history of free-swimming and sessile lifestyles in urochordates as deduced from 18S rDNA molecular phylogeny. *Molecular Biology and Evolution*, *15*, 1189–1194.

SUPPORTING INFORMATION

Additional supporting information can be found online in the Supporting Information section at the end of this article.

How to cite this article: Zemann, B., Le, M.-L. V., Sherlock, R. E., Baum, D., Katija, K., & Stach, T. (2023). Evolutionary traces of miniaturization in a giant—Comparative anatomy of brain and brain nerves in *Bathochordaeus stygius* (Tunicata, Appendicularia). *Journal of Morphology*, *284*, e21598. https://doi.org/10.1002/jmor.21598